

AFFTC-PA-11250



# A NEW APPROACH TO MULTIPATH MITIGATION IN AERONAUTICAL TELEMETRY

Michael Rice,  
Gayatri Narumanchi,  
Mohammad Saquib

AIR FORCE FLIGHT TEST CENTER  
EDWARDS AFB, CA

June 23, 2011

Approved for public release; distribution is unlimited.

AIR FORCE FLIGHT TEST CENTER  
EDWARDS AIR FORCE BASE, CALIFORNIA  
AIR FORCE MATERIEL COMMAND  
UNITED STATES AIR FORCE

A  
F  
F  
T  
C



# **A NEW APPROACH TO MULTIPATH MITIGATION IN AERONAUTICAL TELEMETRY**

**Michael Rice**  
Brigham Young University  
Provo, Utah, USA

**Gayatri Narumanchi, Mohammad Saquib**  
The University of Texas at Dallas  
Richardson, Texas, USA

## **ABSTRACT**

This paper compares the bit error rate performance of a single channel equalizer with the bit error rate performance of a multi-channel equalizer (in the form of the time-reversed space-time block code) using channels derived from multipath channel measurements at Edwards AFB, California, and Cairns Army Airfield, Ft. Rucker, Alabama. The results show that the performance of the multi-channel equalizer is better than the single channel equalizer over the weaker channel, but worse than the performance of the single channel equalizer over the stronger channel. We conclude that the best approach for the informed transmitter is to apply all available power to a single antenna, whereas the best approach for the uninformed transmitter is to apply equal power with transmit diversity to the two available antennas.

## **INTRODUCTION**

Multipath propagation is a fact of life for any wireless communications link. This is especially true in aeronautical telemetry where the need to push ever-increasing amounts of data to the ground is increasing the bandwidth of the modulated carrier. As bandwidth increases, the multipath propagation environment becomes more frequency selective [1] and multipath interference becomes the dominant link impairment.

To understand multipath propagation, its effects on a telemetry downlink, and the performance of multipath mitigation techniques, a number of multipath channel sounding experiments have been conducted over the past decade. For “up and away” flight profiles, the relatively narrow beamwidth of the ground-based receive antenna tends to attenuate off-boresite reflections in the propagation path. However, low-elevation-angle and flight-line scenarios present serious challenges. Previous

work in this area of low-elevation angle “up and away” scenarios include experiments conducted at the Air Force Flight Test Center, Edwards Air Force Base, in L- and S-bands [2] and at Pt. Mugu Naval Air Station over the Pacific Ocean in X-band [3]. These experiments provided useful data for low-elevation-angle propagation in the “up and away” scenario at test ranges in the western United States. Flight-line data, collected from a helicopter-to-ground link along the flight-line at Cairns Army Airfield, Ft. Rucker, Alabama, [4] provides data for flight-line propagation.

This multipath propagation information can be used to assess the effectiveness of multipath mitigation techniques. Multipath mitigation techniques may be broadly categorized as diversity or equalization methods. Diversity techniques have had limited appeal in aeronautical telemetry due to cost – the expense of using more than one (expensive) tracking antenna to realize spatial diversity on the ground and the cost of additional bandwidth required to realize frequency and temporal diversity. Consequently, little work has been done to consider the impact of using spatial diversity to improve the link.<sup>1</sup> As a result, equalization techniques have received the most attention [22] – [28]. However, the emphasis in this prior work has been on blind and adaptive techniques, and the reported results present a relatively weak case for using such techniques in aeronautical telemetry.

Motivated by these results, this paper explores the combined use of multiple transmit antennas and equalization, in the form of a time-reversed space-time block code (TR-STBC) [29, 30]. We apply the equalizers to SOQPSK operating over two example channels: the 2-ray channel whose model is applicable to up and away flight paths at Edwards AFB [2] and multi-channel flight-line channel impulse responses captured at Cairns Army Airfield, Ft. Rucker, Alabama [4].

A comparison of the bit error rate performance of signal channel equalizers with the bit error rate performance of TR-STBC equalization shows that the performance of TR-STBC is *between* the performance of the two corresponding signal channel equalizers. In other words, the performance of TR-STBC is better than the single channel equalizer over the weaker channel, but worse than the performance of the single channel equalizer over the stronger channel. We conclude that the best approach for the informed transmitter is to apply all available power to a single antenna, whereas the best approach for the uninformed transmitter is to apply equal power with TR-SRBC to the two available antennas.

## EQUALIZATION WITH SOQPSK

In this section we explain the equalizer used to generate the results. The first step in developing the equalizer is understanding the relationship between an unequalized SOQPSK system in the additive white Gaussian noise environment and the an equalized SOQPSK system in the presence

---

<sup>1</sup>Essentially all of the work in spatial diversity in aeronautical telemetry has been devoted to *selection diversity* (selecting the best signal from a number [usually two] of different antenna feeds). Turner and Potter [5] describe a telemetry ground station in Japan using two antennas and selection diversity. Several papers describe methods for identifying the best signal from hypothetical antennas. See [6] – [11]. Best Source Selection is a bit level version of the selection diversity concept and has received the most attention. See [12] – [21]. Because it operates on the recovered bit streams, it can be thought of as “poor man’s” selection diversity. In most cases, best source selection is applied when the multiple receive antennas are too far apart to allow any realistic application of the signal-based diversity techniques.

of channel distortion. The additive white Gaussian noise system is illustrated in Figure 1 (a). The SOQPSK source produces an I/Q baseband version (usually called the complex-valued low-pass equivalent [1]) of an SOQPSK signal labeled  $s(t)$ . The received signal is  $r(t) = s(t) + n(t)$  where  $n(t)$  represents the additive thermal noise produced by the receiver. The demodulator used in this paper is an ideal low-pass filter that passes  $s(t)$  unchanged, but bandlimits the noise. The output of the low-pass filter,  $y(t)$ , is sampled at 1 sample per bit (i.e., one sample each  $T_b$  seconds) to produce the discrete-time sequence  $y(kT_b)$ . This discrete-time sequence may be expressed as

$$y(kT_b) = s(kT_b) + n(kT_b) \quad (1)$$

where  $s(kT_b)$  are  $T_b$ -spaced samples of the SOQPSK signal and  $n(kT_b)$  are samples of the low-pass filtered noise process. The sampled low-pass filter outputs are used by the decision device to make the bit decision  $\hat{b}_k$  using the following rule:

$$\hat{b}_k = \begin{cases} 1 & \text{Re}[y(kT_b)] \geq 0 \\ 0 & \text{otherwise} \end{cases} \quad k = \text{even} \quad \hat{b}_k = \begin{cases} 1 & \text{Im}[y(kT_b)] \geq 0 \\ 0 & \text{otherwise} \end{cases} \quad k = \text{odd} \quad (2)$$

An example of an equalized SOQPSK system is illustrated in Figure 1 (b). Here, the SOQPSK signal  $s(t)$  passes through a channel with impulse response  $h(t)$  before arriving at the receiver. The channel models the filtering and multipath propagation. In this case, the received signal is

$$r(t) = s(t) * h(t) + n(t) \quad (3)$$

where  $*$  represents the convolution operation and  $n(t)$  is the thermal receiver noise as before. The idealized demodulator, consisting of an ideal low-pass filter and a sampler are applied to the received signal. The resulting sequence  $y(kT_b)$  may be expressed as

$$y(kT_b) = h(kT_b) * s(kT_b) + n(kT_b) \quad (4)$$

where  $h(kT_b)$  are  $T_b$ -spaced samples of the low-pass filtered channel impulse response  $h(t)$ ,  $*$  denotes discrete-time convolution,  $s(kT_b)$  are  $T_b$ -spaced samples of the SOQPSK signal, and  $n(kT_b)$  are samples of the low-pass filter noise process. The sequence  $y(kT_b)$  is applied to a discrete-time system, called an equalizer, to remove the distortion caused by  $h(t)$ . The output of the equalizer,  $z(kT_b)$ , is applied to the decision device whose bit decisions are

$$\hat{b}_k = \begin{cases} 1 & \text{Re}[z(kT_b)] \geq 0 \\ 0 & \text{otherwise} \end{cases} \quad k = \text{even} \quad \hat{b}_k = \begin{cases} 1 & \text{Im}[z(kT_b)] \geq 0 \\ 0 & \text{otherwise} \end{cases} \quad k = \text{odd} \quad (5)$$

In the context of equalizers, it is often helpful to express the equalizer input (4) using vector/matrix notation. Assuming the received data corresponds to  $N$  bits and that the bandlimited discrete-time

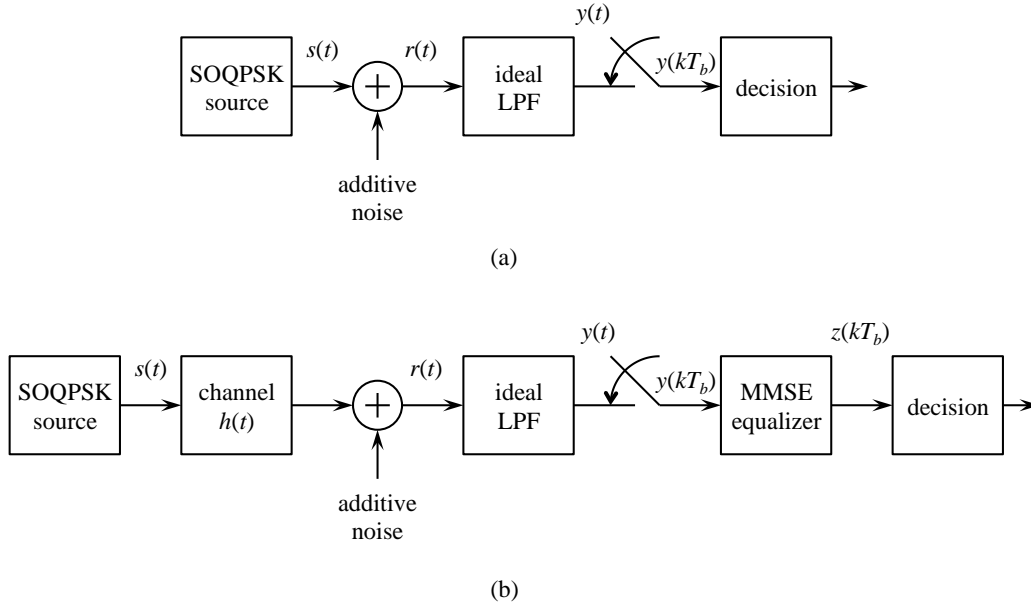


Figure 1: The SOQPSK systems used in this paper: (a) The SOQPSK system in the AWGN environment with an idealized demodulator; (b) The SOQPSK system with an MMSE equalizer in a multipath environment.

channel has support on the interval  $-K_1 \leq k \leq K_2$ , we have

$$\begin{bmatrix} y(0) \\ y(T_b) \\ y(2T_b) \\ \vdots \\ y((N-1)T_b) \end{bmatrix} = \begin{bmatrix} h(0) & h(-T_b) & h(-2T_b) & \cdots & 0 \\ h(T_b) & h(0) & h(-T_b) & \cdots & 0 \\ h(2T_b) & h(T_b) & h(0) & \cdots & 0 \\ \vdots & \vdots & \vdots & \ddots & \vdots \\ 0 & \cdots & \cdots & h(0) & 0 \end{bmatrix} \begin{bmatrix} 0 \\ s(0) \\ s(T_b) \\ s(2T_b) \\ \vdots \\ s((N-1)T_b) \\ 0 \end{bmatrix} + \begin{bmatrix} n(0) \\ n(T_b) \\ n(2T_b) \\ \vdots \\ n((N-1)T_b) \end{bmatrix}$$

which may be expressed as

$$\mathbf{y} = \mathbf{H}\mathbf{s} + \mathbf{n} \quad (6)$$

where  $\mathbf{y}$  is an  $N \times 1$  vector containing the sampled low-pass filter outputs,  $\mathbf{H}$  is an  $(N + K_1 + K_2) \times N$  convolution matrix formed from  $T_b$ -spaced samples of the filtered channel impulse response,  $\mathbf{s}$  is an  $(N + K_1 + K_2) \times 1$  vector containing  $N$   $T_b$ -spaced samples of the SOQPSK signal with  $K_1$  prepended zeros and  $K_2$  appended zeros, and  $\mathbf{n}$  is an  $N \times 1$  vector containing  $T_b$ -spaced samples of the filtered noise.

Of the many criteria that could be used to design the equalizer, we use the minimum mean-squared error criteria in this paper. This serves to demonstrate the potential effectiveness of equalizers with SOQPSK over channels encountered in aeronautical telemetry. In this paper, the MMSE equalizer filter is represented by the  $N \times N$  linear operator  $\mathbf{C}$ . The vector of equalized outputs is

$$\mathbf{z} = \mathbf{C}\mathbf{y} \quad (7)$$

where  $\mathbf{z}$  is an  $N \times 1$  vector containing equalizer output  $z(0), z(T_b), z(2T_b), \dots, z((N-1)T_b)$ . Based on the MMSE criterion, the linear operator representing the MMSE equalizer is

$$\mathbf{C} = \left( \mathbf{H}^\dagger \mathbf{H} + \frac{\sigma_n^2}{\sigma_s^2} \mathbf{I} \right)^{-1} \mathbf{H}^\dagger \quad (8)$$

where  $\mathbf{H}^\dagger$  is the Hermitian (conjugate-transpose) operation,  $\sigma_n^2$  is the variance of the noise samples, and  $\sigma_s^2$  is the variance of the SOQPSK samples.

The reader should be reminded that the equalizer (8) used with the system of Figure 1 (b) is an idealized abstraction. The system is ideal for the following reasons:

1. The low-pass filter passes the SOQPSK signal unchanged while simultaneously bandlimiting the noise in such a way that its  $T_b$ -spaced samples are uncorrelated. This is not true in a real system. In fact, symbol-by-symbol detectors employ a detection filter to minimize the probability of bit error in the AWGN environment [31]. These detection filters alter the SOQPSK samples and correlate the noise.
2. The equalizer possesses perfect knowledge of the sampled channel impulse response. In practice, the channel impulse response must be estimated from the received signal. The estimate is rarely perfect and can degrade the resulting bit error rate performance.

Even with these idealizations, the results of this paper can be used to assess the promise of the single channel equalizer and the multiple channel equalizer (described below). For example, if the equalization results for the idealized case are not promising, there is little reason to pursue the idea further. Fortunately, the results *are* promising and this promise serves as the motivation for thinking about actual systems that are as close as possible to the idealized system.

As explained in the introduction, the experiments with SOQPSK and single channel equalizers has been inconclusive and that this lack of a clear advantage motivates the investigation of multichannel equalization techniques. The most applicable multi-channel equalizer is based on a time-reversed space-time block code (TR-STBC) [29, 30]. The operation of the TR-STBC is based on a system involving two transmit antennas, called transmit antenna 1 and transmit antenna 2, and one receive antenna as illustrated in Figure 2. The starting point for the TR-STBC is a block of  $2N$  data bits. The encoding procedure may be described as follows:

1. Divide the block of bits into 2 length- $N$  bit sequences (say, the first  $N$  bits and the second  $N$  bits). Produce the SOQPSK signal corresponding to the first sequence of  $N$  bits and call it  $s_1(t)$ . Produce the SOQPSK signal corresponding to the second sequence of  $N$  bits and call it  $s_2(t)$ .
2. During the first time slot of duration  $NT_b$ , transmit  $s_1(t)$  from transmit antenna 1 and  $s_2(t)$  from transmit antenna 2.
3. Insert a guard time corresponding to the length of the channel impulse response.
4. During the second time slot of duration  $NT_b$ , transmit  $s_2^*(-t)$  from transmit antenna 1 and  $-s_1^*(-t)$  from transmit antenna 2.

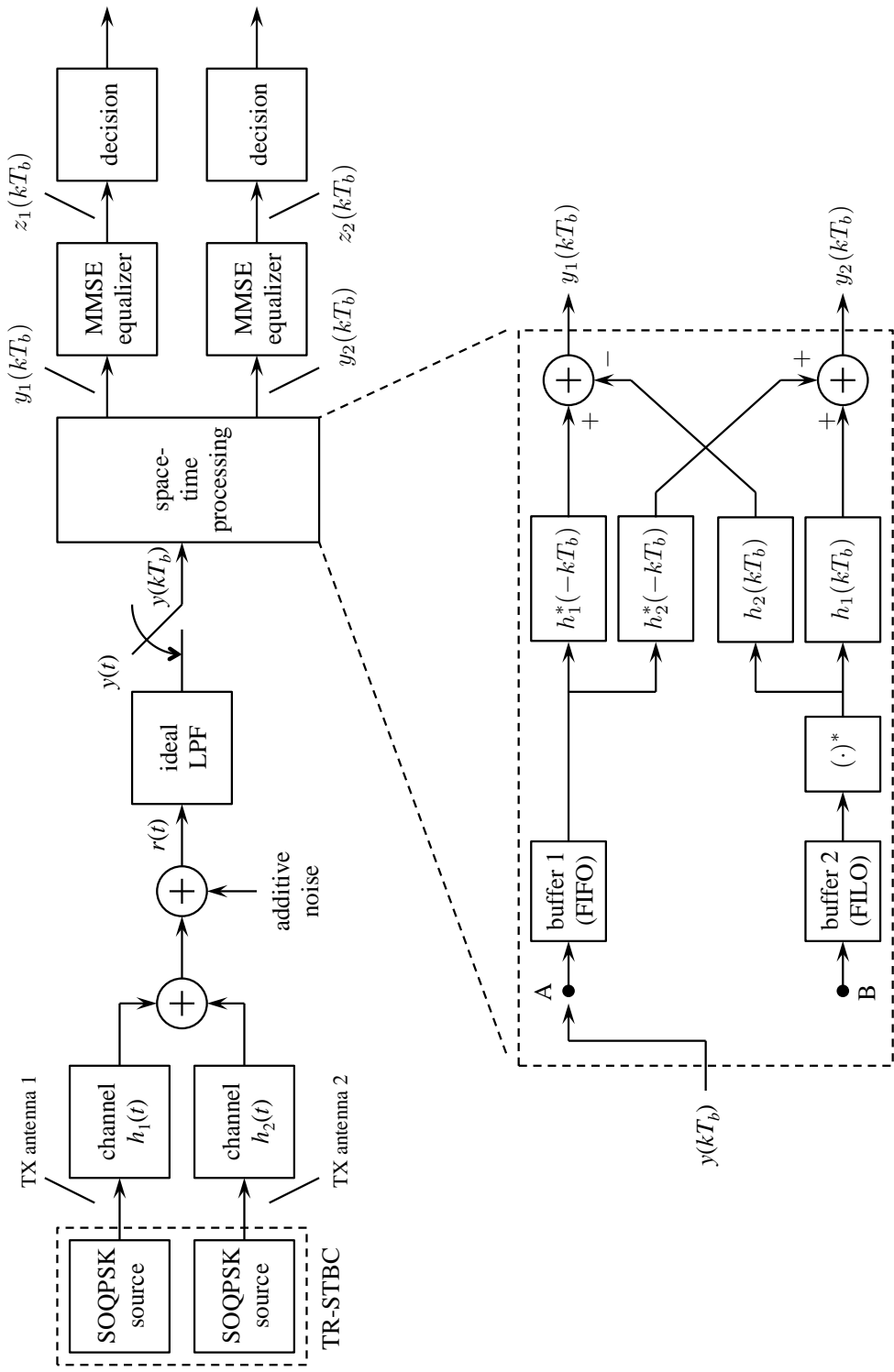


Figure 2: A block diagram of the SOQPSK system using time-reversed space-time block codes (TR-STBC) with a system of 2 transmit antennas and 1 receive antenna.

At the receiver, the signal received during the first time slot is

$$r_1(t) = h_1(t) * s_1(t) + h_2(t) * s_2(t) + n_1(t) \quad (9)$$

where  $h_1(t)$  and  $h_2(t)$  are the impulse responses of the channels between the receiver and transmit antennas 1 and 2, respectively and  $n_1(t)$  is the thermal receiver noise during the first time slot. During the second time slot, the received signal is

$$r_2(t) = h_1(t) * s_2^*(-t) - h_2(t) * s_1^*(-t) + n_2(t) \quad (10)$$

where  $n_2(t)$  is the thermal receiver noise during the second time slot.

The same ideal low-pass filter and sampler are used for the demodulator. The sampled low-pass filter output creates two blocks of samples that are processed by the space-time processing block shown in the figure. The space-time processing block performs spatio-temporal matched filtering and produces two blocks of data  $y_1(kT_b)$  and  $y_2(kT_b)$  given by

$$\begin{aligned} y_1(kT_b) &= h_{\text{eq}}(kT_b) * s_1(kT_b) + v_1(kT_b) \\ y_2(kT_b) &= h_{\text{eq}}(kT_b) * s_2(kT_b) + v_2(kT_b) \end{aligned} \quad (11)$$

where

$$h_{\text{eq}}(kT_b) = h_1(kT_b) * h_1^*(-kT_b) + h_2(kT_b) * h_2^*(-kT_b) \quad (12)$$

is the equivalent channel produced by the spatio-temporal processing;  $s_1(kT_b)$  and  $s_2(kT_b)$  are  $T_b$ -spaced samples of  $s_1(t)$  and  $s_2(t)$ , respectively; and  $v_1(kT_b)$  and  $v_2(kT_b)$  are the responses of the spatio-temporal processing to the samples of the thermal noise processes. The random sequence  $v_1(kT_b)$  is a zero-mean complex-valued Gaussian random sequence with autocorrelation function  $\sigma_n^2 h_{\text{eq}}(kT_b)$ . The random sequence  $v_2(kT_b)$  has the same statistics as  $v_1(kT_b)$ , but is uncorrelated with  $v_1(kT_b)$ . In this way, the spatio-temporal processing creates statistically decoupled versions of  $s_1(kT_b)$  and  $s_2(kT_b)$ . For this reason, equalization may be applied to  $y_1(kT_b)$  and  $y_2(kT_b)$  independently and in parallel as shown. Because both  $y_1(kT_b)$  and  $y_2(kT_b)$  “see” the same channel, the same equalizer may be applied to both.

The equalizer inputs may be represented using the vector/matrix notation introduced above. Let

$$\begin{aligned} \mathbf{y}_1 &= \begin{bmatrix} y_1(0) \\ y_1(T_b) \\ y_1(2T_b) \\ \vdots \\ y_1((N-1)T_b) \end{bmatrix}, \mathbf{y}_2 = \begin{bmatrix} y_2(0) \\ y_2(T_b) \\ y_2(2T_b) \\ \vdots \\ y_2((N-1)T_b) \end{bmatrix}, \\ \mathbf{s}_1 &= \begin{bmatrix} s_1(0) \\ s_1(T_b) \\ s_1(2T_b) \\ \vdots \\ s_1((N-1)T_b) \end{bmatrix}, \mathbf{s}_2 = \begin{bmatrix} s_2(0) \\ s_2(T_b) \\ s_2(2T_b) \\ \vdots \\ s_2((N-1)T_b) \end{bmatrix}, \end{aligned}$$

$$\mathbf{v}_1 = \begin{bmatrix} v_1(0) \\ v_1(T_b) \\ v_1(2T_b) \\ \vdots \\ v_1((N-1)T_b) \end{bmatrix}, \mathbf{v}_2 = \begin{bmatrix} v_2(0) \\ v_2(T_b) \\ v_2(2T_b) \\ \vdots \\ v_2((N-1)T_b) \end{bmatrix},$$

and

$$\mathbf{H}_1 = \begin{bmatrix} h_1(0) & h_1(-T_b) & h_1(-2T_b) & \cdots & 0 \\ h_1(T_b) & h_1(0) & h_1(-T_b) & \cdots & 0 \\ h_1(2T_b) & h_1(T_b) & h_1(0) & \cdots & 0 \\ \vdots & & & & \vdots \\ 0 & & & \cdots & h_1(0) \end{bmatrix}$$

$$\mathbf{H}_2 = \begin{bmatrix} h_2(0) & h_2(-T_b) & h_2(-2T_b) & \cdots & 0 \\ h_2(T_b) & h_2(0) & h_2(-T_b) & \cdots & 0 \\ h_2(2T_b) & h_2(T_b) & h_2(0) & \cdots & 0 \\ \vdots & & & & \vdots \\ 0 & & & \cdots & h_2(0) \end{bmatrix}.$$

The vectors  $\mathbf{y}_1$  and  $\mathbf{y}_2$  may be expressed as

$$\mathbf{y}_1 = \mathbf{H}_{\text{eq}}\mathbf{s}_1 + \mathbf{v}_1 \quad \mathbf{y}_2 = \mathbf{H}_{\text{eq}}\mathbf{s}_2 + \mathbf{v}_2 \quad (13)$$

where

$$\mathbf{H}_{\text{eq}} = \mathbf{H}_1^\dagger \mathbf{H}_1 + \mathbf{H}_2^\dagger \mathbf{H}_2 \quad (14)$$

is the convolution matrix corresponding to the equivalent channel seen by each of the equalizers. The MMSE equalizers may be represented by the linear operator

$$\mathbf{C} = \left( \mathbf{H}_{\text{eq}} + \frac{\sigma_n^2}{\sigma_s^2} \mathbf{I} \right)^{-1}. \quad (15)$$

The vectors containing the decision device inputs are

$$\mathbf{z}_1 = \mathbf{C}\mathbf{y}_1 \quad \mathbf{z}_2 = \mathbf{C}\mathbf{y}_2 \quad (16)$$

## EQUALIZATION RESULTS

As examples, we consider a 10-Mbit/s SOQPSK telemetry link operating in two different multipath environments. The first environment is based on the two channels plotted in Figure 7 and derived from geometric considerations following the wideband aeronautical telemetry channel described in [2]. The details associated with the channels are described in the Appendix. The second environment is based on the flight-line channels captured at Cairns Army Airfield, Ft. Rucker, Alabama [4]. The multipath channel impulse responses are plotted in Figure 11. Some background information on these channels is described in the Appendix.

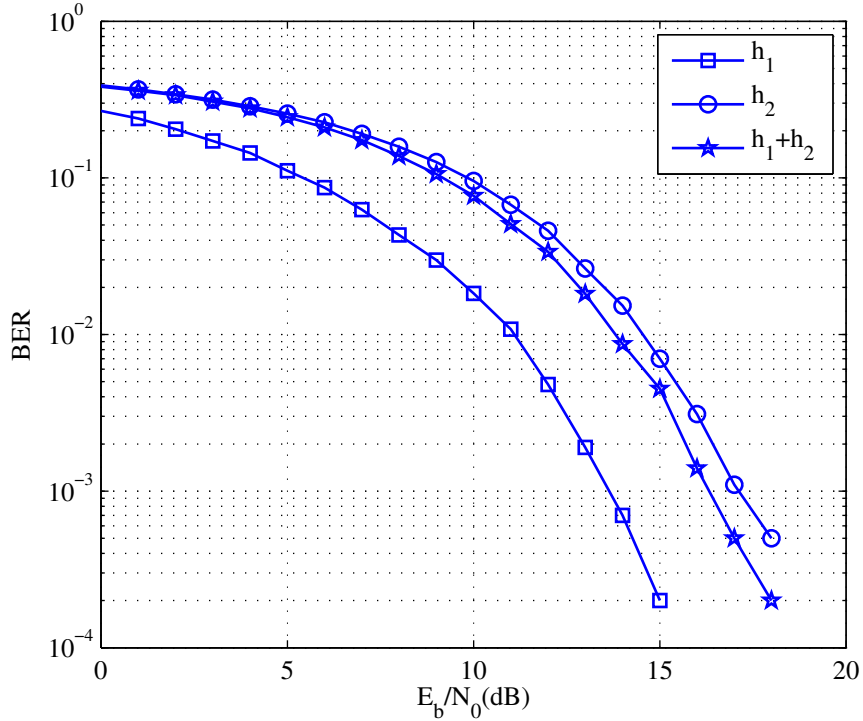


Figure 3: Simulated bit error rate performance for equalized SOQPSK over the two 2-ray channels plotted in Figure 7.

The simulated bit error rate (BER) performance for the channels plotted in Figure 7 are shown in Figure 3. In this figure, the box and circle markers quantify the bit error rate performance of the single channel system of Figure 1 (b) using the MMSE equalizer (8) over channels  $h_1$  and  $h_2$ , respectively. We observe that the BER performance over channel  $h_1$  is much better than the BER performance over channel  $h_2$ . This is to be expected based on the frequency domain plots of Figure 8. These plots show that the frequency null for channel  $h_2$  is much closer to the carrier frequency than the null for channel  $h_1$ . The BER performance of the TR-STBC technique (see Figure 2) applied to these two channels and using the equalizer (15) is marked by the stars. Curiously, the bit error rate performance of the TR-STBC system is *worse* than the system using only  $h_1$  by about 3 dB but better than the system using only  $h_2$  by about 1 dB. This is due to the fact that full power is applied to either  $h_1$  or  $h_2$  in the single channel case, but only half power is applied to each channel in the TRSTBC case.

The simulated BER performance for the three channels plotted in Figure 11 are shown in Figure 4. In this figure the clear markers quantify the BER performance of the single channel system of Figure 1 (b) using the MMSE equalizer (8). Observe that the equalized BER performance over channel  $h_4$  is much better than that the equalized BER performance over channel  $h_1$ . (The equalized BER performance over channel  $h_3$  is in between the two.) The BER performance of the TR-STBC technique applied to the three possible combinations of two channels are marked by the solid markers. Each pairing of channels presents to the system unequal channels, one of the two is better than the other. The simulation results show that the equalized BER performance of the TR-STBC system

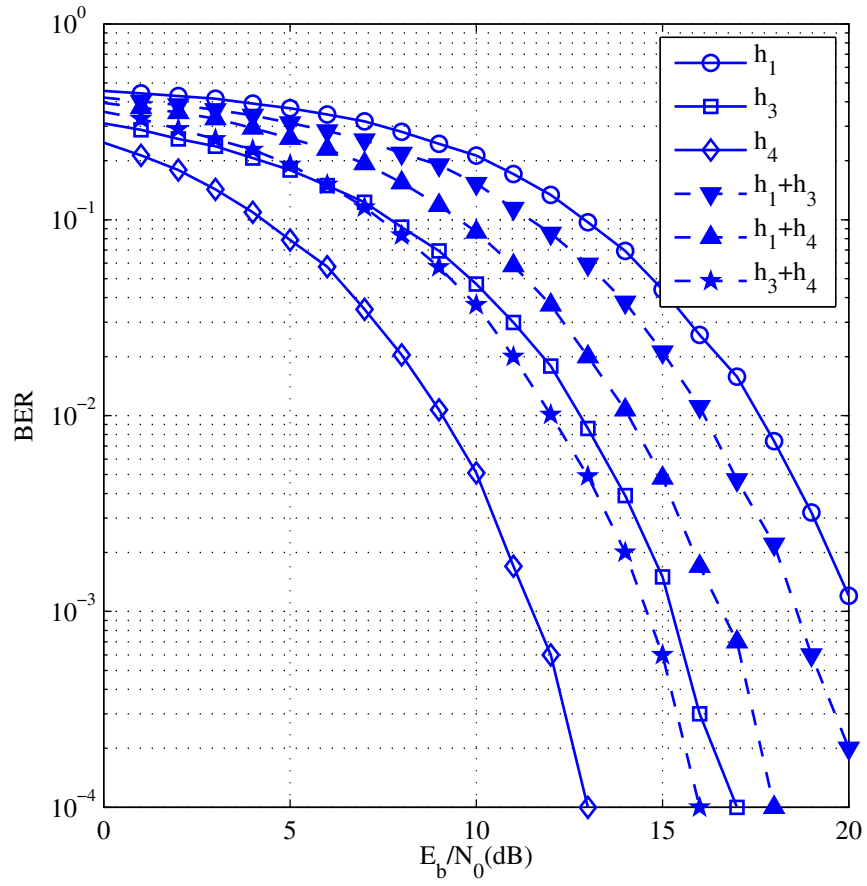


Figure 4: Simulated bit error rate performance for equalized SOQPSK over the three channels plotted in Figure 11.

is always in between the performance curves for the corresponding single channel systems. As before, the single channel systems apply full power to the transmit antenna whereas the TR-STBC system applies half power to each of the two transmit antennas.

## CONCLUSIONS

The simulation results summarized in the previous section show that the equalization can improve the bit error rate performance over representative channels found in aeronautical telemetry. The results presented here are better than those presented earlier in [22] – [28] primarily because the equalizer knows the channel. Multi-channel equalization, in the form of a time-reversed space-time block code (TR-STBC) was also explored and the simulated bit error rate performance was compared to that of the equalized single channel counterparts. The results show that the BER performance of the TR-STBC is in between that of the two single channel systems. At first sight, these results might appear to make a case *against* the use of TR-STBC. This conclusion would be the correct one if the airborne transmitter *knew* which of its antennas had the best propagation path to the receiver. This is called the *informed transmitter* scenario. The optimum approach for the informed transmitter appears to be the application of all available power to the antenna with the best propagation path to the receiver. On the other hand, if the airborne transmitter does not know which antenna has the best propagation path to the receiver, the only option is to apply power to each antenna and apply signaling that injects some diversity into the system. This is the role of the TR-STBC.

## APPENDIX

### A. *The 2-Ray Channel (EAFB)*

The 2-ray channel used for the equalizer simulations is based on the wideband channel model described in [2]. This model is based on the geometry defined by the airborne transmitter, the ground-based receiver, and the terrain features. The geometry is illustrated in Figures 5 and 6. Figure 5 shows the aircraft at a point on the Cords Road flight corridor near Edwards AFB. The assumed altitude is 5000' AMSL. The receiver is Building 5790 located on a small hill top at an altitude of 2966' AMSL. The reflecting surface is at an altitude of 2300' AMSL. The diagram shown in Figure 6 illustrates the geometry of the multipath propagation for this scenario. The propagation environment is dominated by a line-of-sight path and a strong “ground bounce.” For the TR-STBC, the two antenna locations are shown on C-12 diagram on the lower portion of Figure 6. This geometry defines two 2-ray paths as shown. Low-pass filtering the resulting 2-ray channels and sampling at 10 Msamples/s (to match the bit rate used in the simulations) produces the complex-valued impulse responses plotted in Figure 7. The corresponding frequency domain representations for the two channels are plotted in Figure 8.

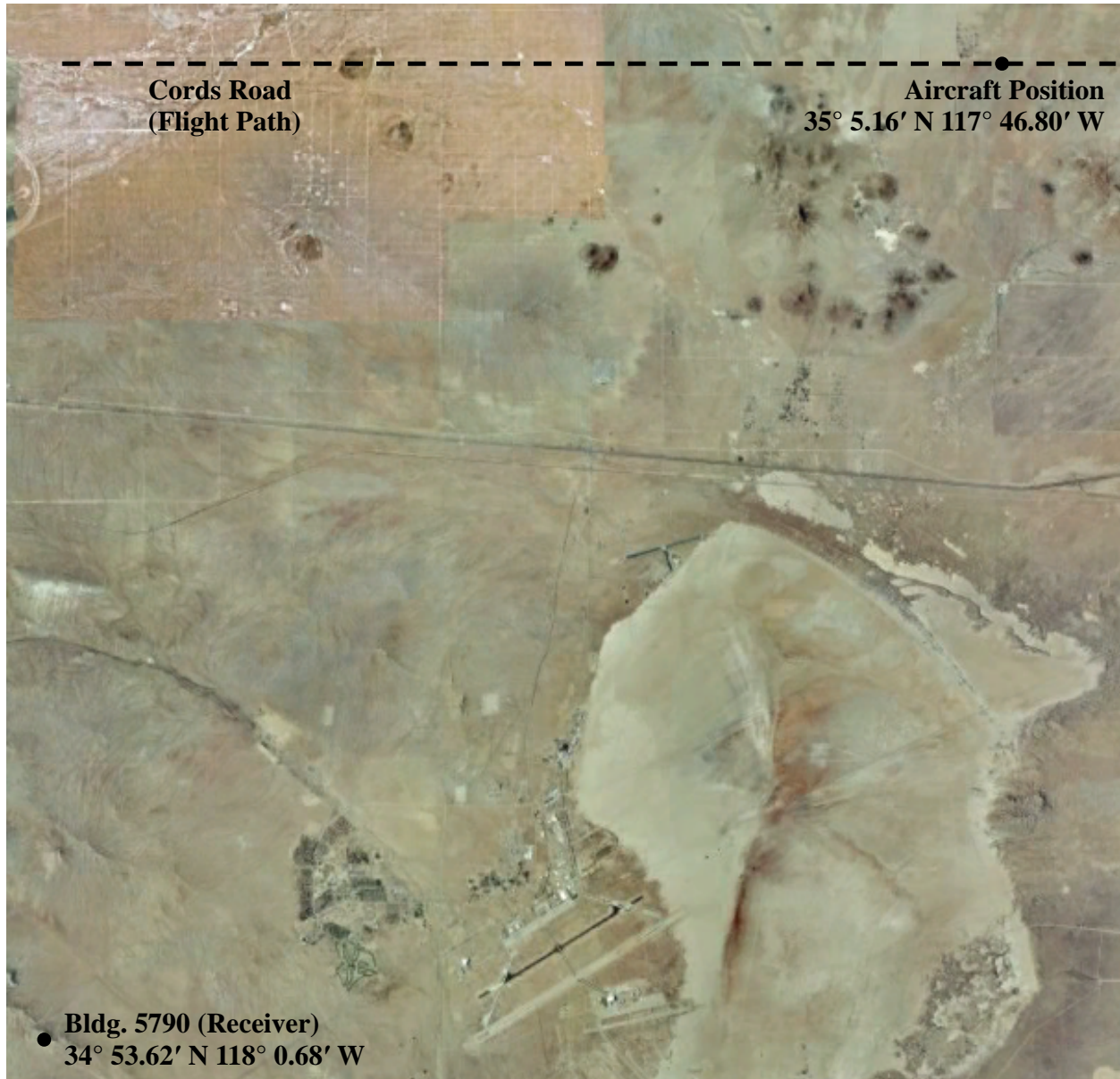


Figure 5: A map showing illustrating the positions used to define the 2-ray channel used in the equalizer simulations.

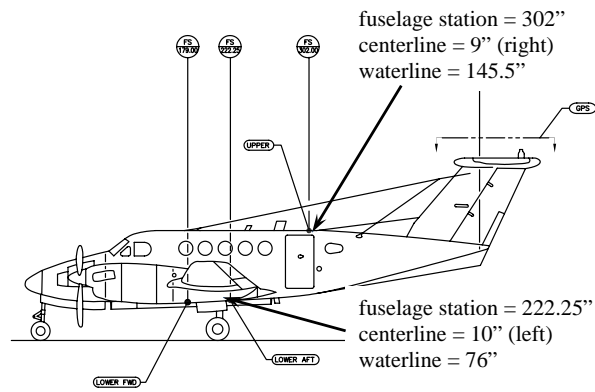
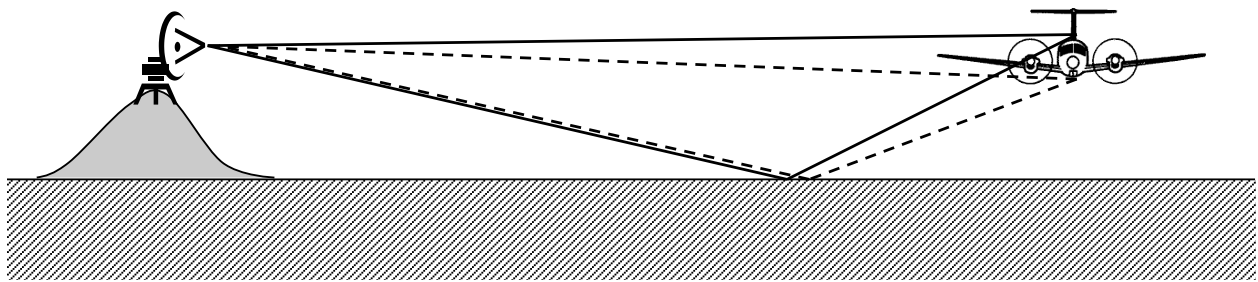


Figure 6: A diagram illustrating the geometry of the 2-ray channel. Compare with the map in Figure 5.

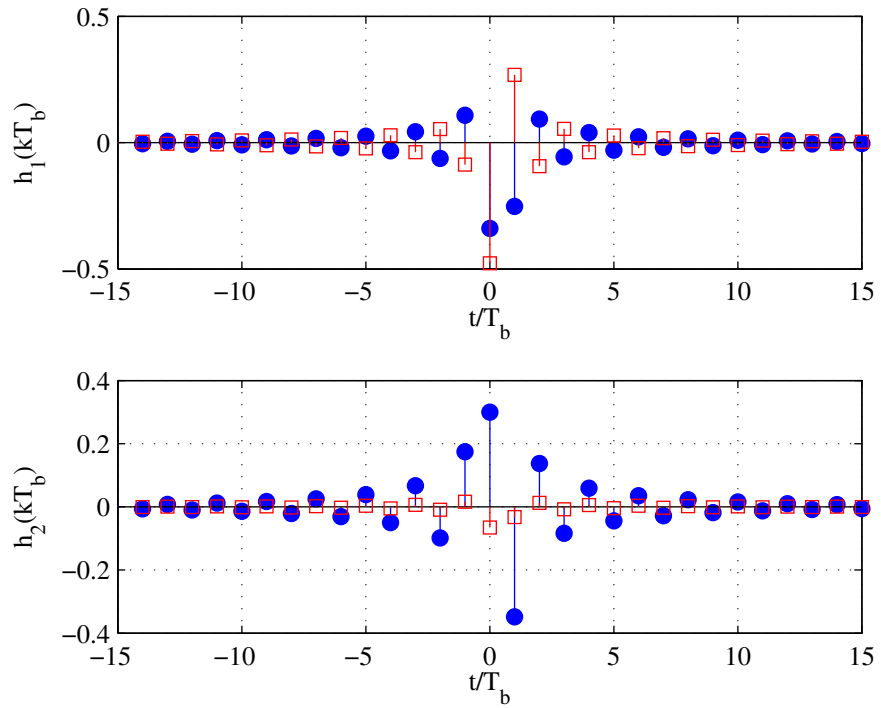


Figure 7: The band-limited discrete-time version of the channel impulse response for the 2-ray channel defined by the geometry of Figures 5 and 6. In these plots, the solid circles represent the real part of the impulse response whereas the clear squares represent the imaginary part of the impulse response.

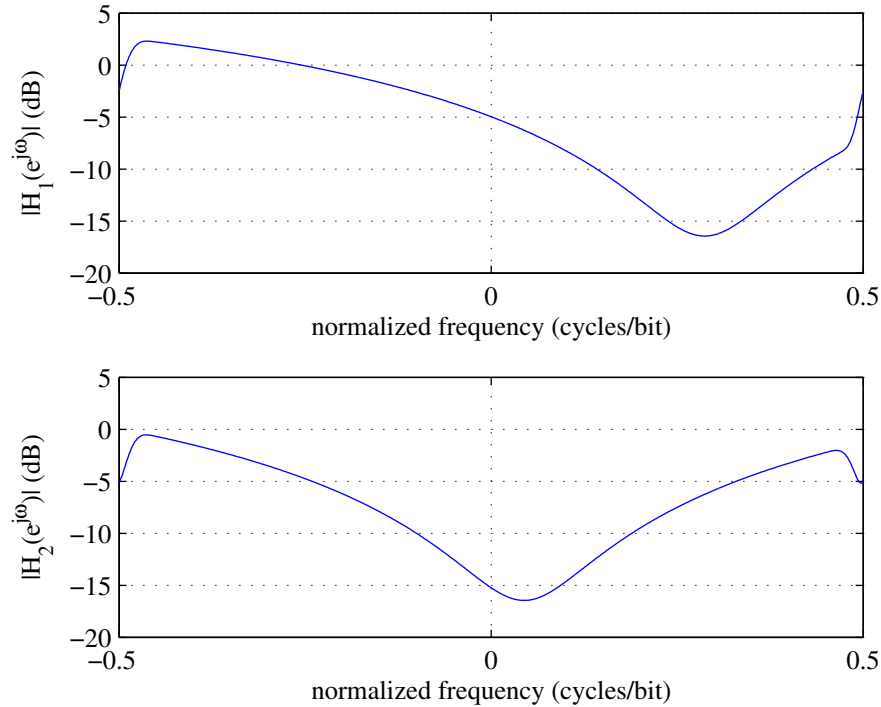


Figure 8: The frequency domain representation of the discrete-time impulse responses plotted in Figure 7.

### B. The Helicopter Flight Line Channel (CAA/Ft. Rucker)

The helicopter flight-line channel is based on channel measurements at Cairns Army Airfield, Ft. Rucker, Alabama. The channel sounding experiments are described in [4]. The airborne transmitter was equipped with three transmit antennas whose locations are shown in Figure 9. Channel impulse responses were captured from three flight-line locations shown in Figure 10. These impulse responses were resampled to 10 Msamples/s to match the bit rate used in the simulations. The time and frequency domain versions of the channels from the top location in Figure 10 are plotted in Figures 11 and 12, respectively.

## ACKNOWLEDGEMENTS

This work was supported by the Test Resource Management Center (TRMC) Test and Evaluation Science and Technology (T&E/S&T) Program through a grant from the US Army Program Executive Office for Simulation, Training, and Instrumentation (PEO STRI) under contract W900KK-09-C-0016. Any opinions, findings and conclusions or recommendations expressed in this material are those of the author and do not necessarily reflect the views of the TRMC and T&E/S&T Program and/or PEO STRI. The Executing Agent and Program Manager work out of the AFFTC.

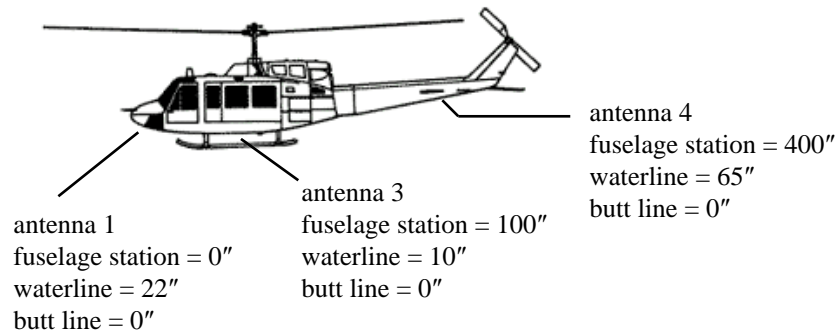


Figure 9: The UH-1H helicopter and the three antenna locations used for the L-band channel sounding experiments at the Cairns Army Airfield, Ft. Rucker, AL.

## REFERENCES

- [1] J. Proakis. *Digital Communications*. McGraw-Hill, 2008.
- [2] M. Rice, A. Davis, and C. Bettwieser. A wideband channel model for aeronautical telemetry. *IEEE Transactions on Aerospace and Electronic Systems*, 40(1):57–69, January 2004.
- [3] Q. Lei and M. Rice. Multipath channel model for over-water aeronautical telemetry. *IEEE Transactions on Aerospace and Electronic Systems*, 45(2):735 – 742, April 2009.
- [4] M. Rice and M. Jensen. Wideband multipath propagation for helicopter-to-ground telemetry links. In *Proceedings of the International Telemetry Conference*, Las Vegas, NV, October 2011.
- [5] W. Turner and R. Potter. Unattended space-diversity telemetry tracking antenna system. In *Proceedings of the International Telemetry Conference*, San Diego, CA, October 1994.
- [6] M. Haghdad and K. Feher. Smart diversity receivers for dynamic, multipath, frequency selective faded FQPSK and other systems. In *Proceedings of the International Telemetry Conference*, Las Vegas, NV, October 2001.
- [7] R. Jefferis. In-service detection of multipath fading. In *Proceedings of the International Telemetry Conference*, San Diego, CA, October 2002.
- [8] M. Haghdad and K. Feher. Pseudo error detection in smart antenna/diversity systems. In *Proceedings of the International Telemetry Conference*, Las Vegas, NV, October 2003.
- [9] R. Jefferis. Telemetry link reliability improvement via “no-hit” diversity branch selection. In *Proceedings of the International Telemetry Conference*, San Diego, CA, October 2004.
- [10] R. Formeister. Diversity branch selection in real world application. In *Proceedings of the International Telemetry Conference*, Las Vegas, NV, October 2007.
- [11] M. Melicher. An enhancement of existing RF data links using advanced diversity techniques. In *Proceedings of the International Telemetry Conference*, San Diego, CA, October 2010.



Figure 10: The three points where channel impulse responses were captured. The receiver is located on a tower at the bottom of the image.

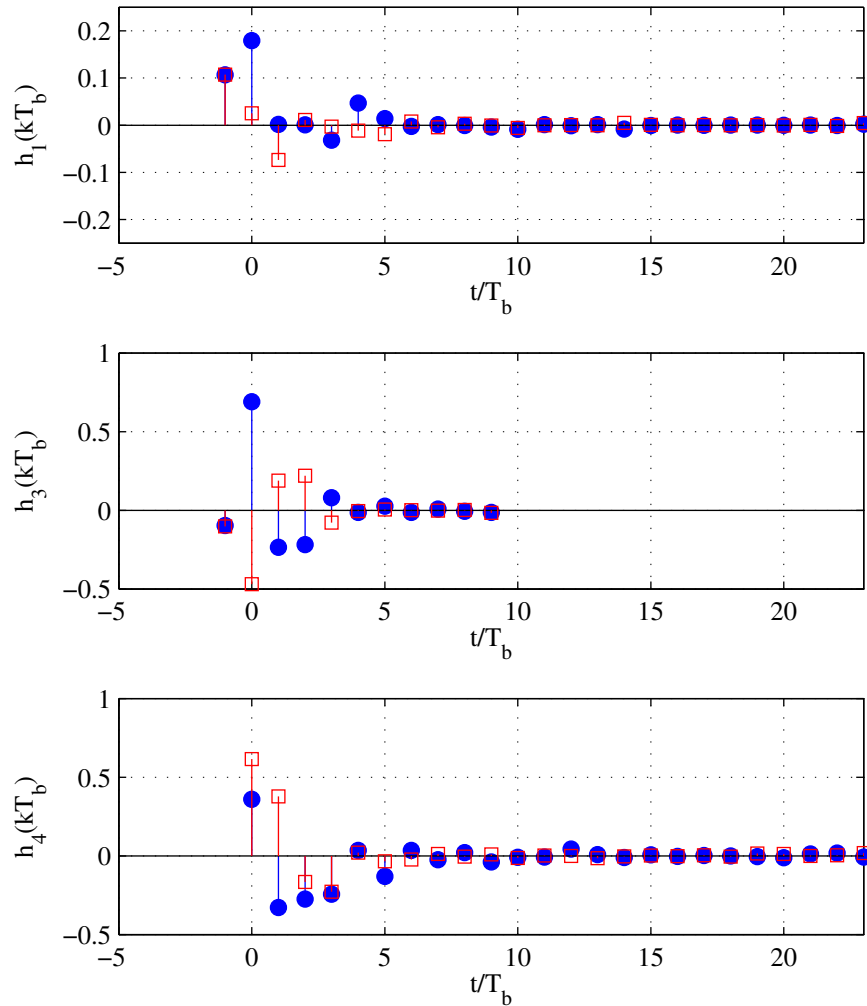


Figure 11: The band-limited discrete-time version of the channel impulse response for the three channels captured at the upper location in Figure 10. The subscripts refer to the antenna numbers shown in Figure 9. In these plots, the solid circles represent the real part of the impulse response whereas the clear squares represent the imaginary part of the impulse response.

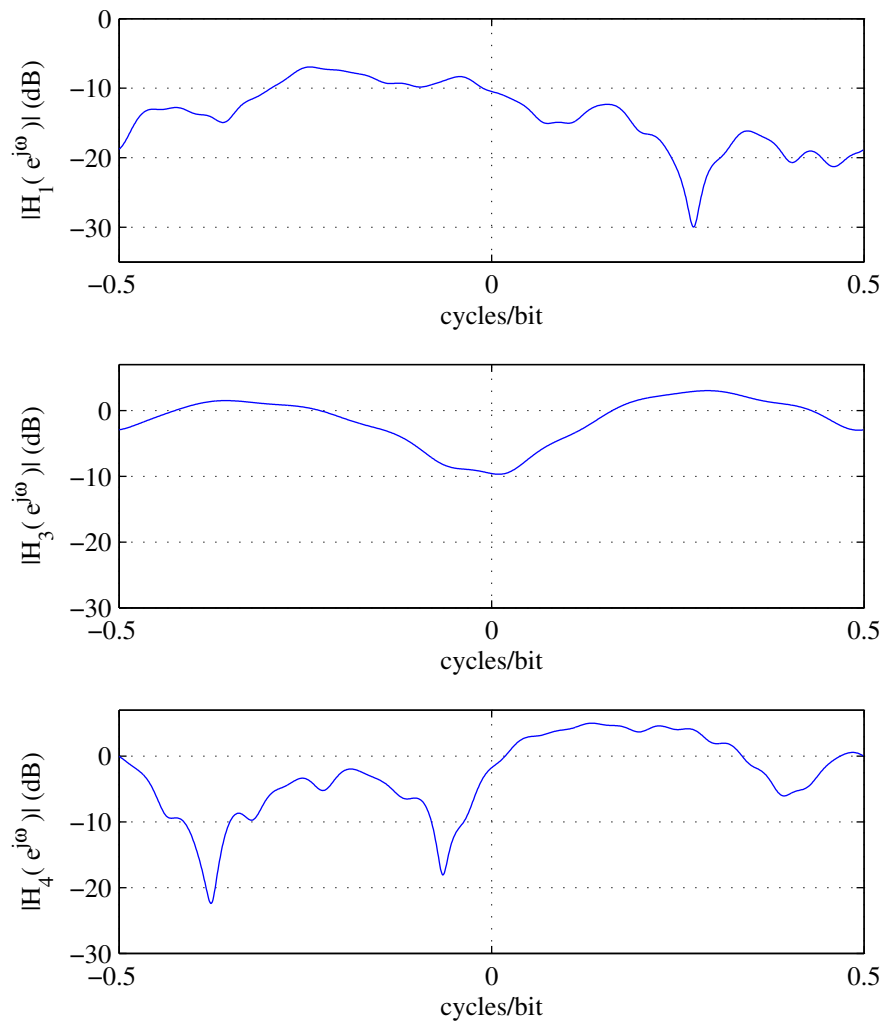


Figure 12: The frequency domain representation of the discrete-time impulse responses plotted in Figure 11.

- [12] D. Peterson. The merging of multisource telemetry data to support over the horizon missile testing. In *Proceedings of the International Telemetry Conference*, Las Vegas, NV, October 1995.
- [13] H. Duffy. Merging of diverse encrypted PCM streams. In *Proceedings of the International Telemetry Conference*, San Diego, CA, October 1996.
- [14] K. Rigley, D. Wheelwright, and B. Fowers. UTTR best telemetry source selector. In *Proceedings of the International Telemetry Conference*, San Diego, CA, October 2000.
- [15] M. Wilson. Merging telemetry data from multiple receivers. In *Proceedings of the International Telemetry Conference*, San Diego, CA, October 2004.
- [16] R. Engler and J. Kirby. Telemetry best source selection at White Sands Missile Range. In *Proceedings of the International Telemetry Conference*, San Diego, CA, October 2004.
- [17] T. Gatton. Best source selectors and measuring the improvements. In *Proceedings of the International Telemetry Conference*, Las Vegas, NV, October 2005.
- [18] E. Reid. Encrypted correlating source selector. In *Proceedings of the International Telemetry Conference*, San Diego, CA, October 2006.
- [19] J. Guradiana. Best source selection on encrypted data. In *Proceedings of the International Telemetry Conference*, San Diego, CA, October 2006.
- [20] C. Fewer and S. Wilmot. Enhancing the PCM/FM link — without the math. In *Proceedings of the International Telemetry Conference*, Las Vegas, NV, October 2007.
- [21] D. Corry. Measuring and evaluating best source selection. In *Proceedings of the International Telemetry Conference*, Las Vegas, NV, October 2009.
- [22] R. Fan, K. Yao, and D. Whiteman. Adaptive equalization for OQPSK through a frequency selective fading channel. In *Proceedings of the International Telemetry Conference*, San Diego, CA, October 2000.
- [23] Z. Ye, E. Satorius, and T. Jedrey. Enhancement of advanced range telemetry (ARTM) channels via blind equalization. In *Proceedings of the International Telemetry Conference*, Las Vegas, NV, October 2001.
- [24] T. Hill and M. Geoghegan. A comparison of adaptively equalized PCM/FM, SOQPSK, and multi-h CPM in a multipath channel. In *Proceedings of the International Telemetry Conference*, San Diego, CA, October 2002.
- [25] M. Geoghegan. Experimental results for PCM/FM, Tier I SOQPSK, and Tier II Multi-h CPM with CMA equalization. In *Proceedings of the International Telemetry Conference*, Las Vegas, NV, October 2003.
- [26] E. Law. How well does a blind adaptive CMA equalizer work in a simulated telemetry multipath environment? In *Proceedings of the International Telemetry Conference*, San Diego, CA, October 2004.

- [27] M. Rice and E. Satorius. A comparison of MMSE and CMA equalization techniques for ARTM Tier-1 waveforms. In *Proceedings of the International Telemetry Conference*, San Diego, CA, October 2004.
- [28] M. Rice and E. Satorius. Equalization techniques for multipath mitigation in aeronautical telemetry. In *Proceedings of the IEEE Military Communications Conference*, Monterey, CA, November 2004.
- [29] E. Lindskog and A. Paulraj. A transmit diversity scheme for channels with intersymbol interference. In *Proceedings of the IEEE International Conference on Communications*, New Orleans, June 2000.
- [30] S. Diggavi, N. Al-Dhahir, and R. Calderbank. Algebraic properties of spacetime block codes in intersymbol interference multiple-access channels. *IEEE Transactions on Information Theory*, 49(10):2403–2414, October 2003.
- [31] M. Geoghegan. Optimal linear detection of SOQPSK. In *Proceedings of the International Telemetry Conference*, San Diego, CA, October 2002.